Available online at www.sciencedirect.com
SCIENCE DIRECT®
Journal of Computational Physics 189 (2003) 493–511
JOURNAL OF COMPUTATIONAL PHYSICS
www.elsevier.com/locate/jcp

PHYSALIS: a new method for particle flow simulation. Part III: convergence analysis of two-dimensional flows

Huaxiong Huang [a,*], Shu Takagi [b]

[a] Department of Mathematics and Statistics, York University, Toronto, Ont., Canada M3J 1P3
[b] Department of Mechanical Engineering, The University of Tokyo, Hongo, Bunkyo-ku, Tokyo 113-8656, Japan

Received 17 October 2001; received in revised form 31 January 2003; accepted 27 March 2003

Abstract

In this paper, we study the convergence property of PHYSALIS when it is applied to incompressible particle flows in two-dimensional space. PHYSALIS is a recently proposed iterative method which computes the solution without imposing the boundary conditions on the particle surfaces directly. Instead, a consistency equation based on the local (near particle) representation of the solution is used as the boundary conditions. One of the important issues needs to be addressed is the convergence properties of the iterative procedure. In this paper, we present the convergence analysis using Laplace and biharmonic equations as two model problems. It is shown that convergence of the method can be achieved but the rate of convergence depends on the relative locations of the cages. The results are directly related to potential and Stokes flows. However, they are also relevant to Navier–Stokes flows, heat conduction in composite media, and other problems.

AMS: 65N12; 76D07; 76T05

Keywords: Particle flows; Potential flows; Stokes flows; Convergence analysis

1. Introduction

Direct numerical simulation of flow around particles has been an active research area due to its relevance to the modeling of multiphase flows and flows in a porous medium. For small particle concentration problems (dilute case), one can solve the flow field by approximating the particles as points [1,3,13]. When the effect of the particle size is not negligible, one has to deal with the boundary conditions on the particle surfaces. Various methods have been proposed in the literature such as the method of fast multipole expansion [12], a fictitious domain method [7,10], the arbitrary Lagrangian–Eulerian (ALE) method [5,6], and a lattice Boltzmann approach [2,4,8,9]. In general, these methods require considerable computer resources.

* Corresponding author. Fax: +416-736-5757.
E-mail addresses: hhuang@yorku.ca (H. Huang), takagi@mech.t.u-tokyo.ac.jp (S. Takagi).

0021-9991/$ - see front matter © 2003 Published by Elsevier Science B.V.
doi:10.1016/S0021-9991(03)00230-4

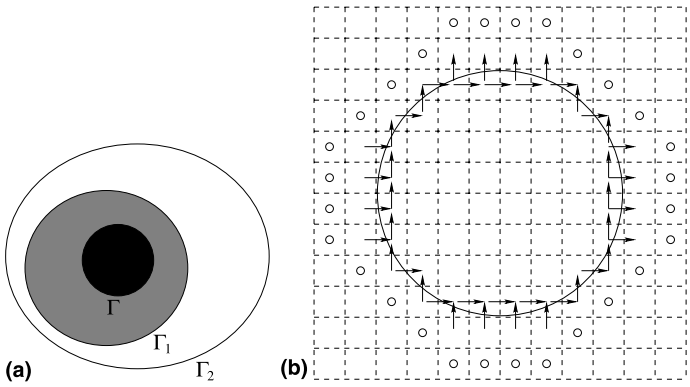

Fig. 1. The setup inner and outer cages near a circular particle surface: (a) continuous case; (b) discrete case, as used in [14]. In the discrete case, the arrows indicate the inner cage velocity points while the circles are on the outer cage.

In [11,14], a new method called PHYSALIS has been successfully applied to three-dimensional potential flows and two-dimensional incompressible viscous flows with nondilute particle concentrations. The basic idea of the method, introduced in [11], can be outlined as follows. Suppose that each particle is enclosed by a surface Γ_1 (Fig. 1(a)) and there exists a local solution $u^{(l_1)}$ valid between Γ_1 and the particle surface Γ. Suppose that $u^{(l_2)}$ is the solution between the particle and a surface Γ_2 which also encloses the particle (Fig. 1(a)), then there exists a consistency equation

$$u^{(l_1)} = F_{12}(u^{(l_2)}) + G_{12}, \tag{1.1}$$

when the problem is linear, as in the case of Laplace equation (for potential flows) and biharmonic equation (for Stokes flows). Here F_{12} and G_{12} are some known functionals. For nonlinear problems such as incompressible flows with a finite Reynolds number, an exact consistency relation may not exist. However, an approximated equation similar to (1.1) often can be found by linearizing the problem. For example, near the no-slip particle surface, the Navier–Stokes equation can be approximated by the Stokes one. Therefore, the method has been applied to nonlinear problems and the analysis presented here is also relevant to those cases.

Since the consistency relation (1.1) implies the satisfaction of the boundary conditions on the particle surface, it can be used to replace the boundary conditions. These surfaces are called the *inner* and *outer cages*, respectively, according to their relative distance from the particle surface. Without the loss of generality, we assume that Γ_1 is the inner cage and Γ_2 is the outer one throughout the rest of the paper. The cages are normally close to the surfaces of the particles but not always outside the particles.

When a standard numerical method such as the finite volume method is used to find the far-field solution, the solution domain is normally covered with a grid. For the ease of implementing (1.1), the surfaces, or the cages, are set up to coincide with the grid points or computational cells where the discrete solutions are stored. An example is shown in Fig. 1(b), in which the cages go through the cell centers and side faces where the velocity or their averaged values are located.

Since the local solutions $u^{(l_1)}$ and $u^{(l_2)}$ are not known a priori, the procedure is necessarily an iterative one, consisting two steps. Firstly, supposed that $u^{(l_1,n)}$, an approximation of the local solution $u^{(l_1)}$ is known. Here the second superscript n denotes the number of iterations. The far-field solution $u^{(f)}$ can be computed using (1.1) on the inner cage as a boundary condition. The value of $u^{(f)}$ on the outer cage is used to construct the local solution $u^{(l_2)}$ afterwards. This provides a functional relationship between the two local solutions, which can be written as

$$u^{(l_2,n)} = F_{21}(u^{(l_1,n)}) + G_{21}, \tag{1.2}$$

where F_{21} and G_{21} are some known functionals. (The details can be found in Sections 2 and 3.) As the second step of the iteration, the consistency equation (1.1) is used to update $u^{(l_1)}$ in the form of

$$u^{(l_1,n+1)} = F_{12}(u^{(l_2,n)}) + G_{12}, \tag{1.3}$$

and the procedure continues. Combine (1.2) and (1.3), we obtain

$$u^{(l_2,n+1)} = H_2(u^{(l_2,n)}) \text{ or } u^{(l_1,n+1)} = H_1(u^{(l_1,n)}), \tag{1.4}$$

which are two related fixed-point iterations for the location solutions. The convergent solutions are therefore the fixed-points of the following equations

$$u^{(l_2)} = H_2(u^{(l_2)}) \text{ or } u^{(l_1)} = H_1(u^{(l_1)}). \tag{1.5}$$

The numerical evidences in [11,14] suggest that the convergence of PHYSALIS in general can be achieved. It is also observed that the method is more robust for potential flows than for Navier–Stokes flows. The main objective of this paper is to present a detailed analysis of the convergence property of the method, under the general framework outline above. The analysis will help us to explain the differences in the performance of the method under various conditions. More importantly, it will enable us to find good strategies for setting up the cages to achieve fast convergence. In order to simplify the analysis, we will only consider a special case in two space dimensions. We will assume that there exists one particle in the entire domain and the particle surface and the far-field boundary are two concentric circles, centered at the original. The cages considered in this study are also circles centered at the original. We will use Laplace and biharmonic equations as two model problems. These two problems have applications not only in fluid flows, but also in other areas such as heat conduction, electro-magnetic fields, and linear elasticity. However, our discussion will be centered on potential and Stokes flows. In addition, we will not be concerned with the specifics of solution methods used to compute the far-field and local solutions and assume that the solutions can be obtained exactly.

With these simplifications, we show that the fixed point iterations (1.4) can be simplified as

$$\vec{U}^{(k,n+1)} = T_k \vec{U}^{(k,n)} + (I - T_k)\vec{U}^{(k)}, \tag{1.6}$$

where T_k are either scalars or 2×2 matrices, $\vec{U}^{(k)}$ are vectors of at most two components, which are coefficients associated with the kth eigensolution, and $\vec{U}^{(k,n)}$ are the values of the nth iteration. Thus the convergence of the method can be analyzed by examining the eigenvalues of T_k, or their spectral radii. Since the iterative matrices T_k depend on the location of the two cages and matching conditions on the cages, the effects of these factors on the speed of convergence can be studied easily.

Our analysis show that for potential flows the best strategy is to use the normal velocity (a Neumann type of condition) on the inner cage to compute the far-field solution and update the coefficients of the eigenfunction expansion of the velocity potential (local solution) by matching the velocity potential directly on the outer cage. Convergence can be achieved as well if the velocity potential is used on both cages while the speed of convergence is slower. Other combinations of matching conditions in general result in poorer convergence (see Section 2). For Stokes flows, the situation is more complicated. If velocity is used on both the inner and outer cages, the iteration only converges when two cages are placed outside the cylinder (particle). On the other hand, when the velocity is used on the inner cage while pressure and vorticity are used on the outer cage, then convergence can be achieved by placing a single cage (i.e., the two cages overlap) inside the cylinder. This corresponds to a strategy that uses the velocity to compute the flow field (far-field solution) but updates the coefficients of the eigenfunction expansion (local solution) with pressure and vorticity on a single cage.

The rest of the paper is organized as follows. In Section 2, we introduce a model problem using Laplace equation. The detailed procedure of PHYSALIS is described first, followed by the convergence analysis. A model problem using the biharmonic equation is investigated in Section 3, which is directly related to Stokes flows but also relevant to Navier–Stokes flows. Detailed discussion of convergence property of the method is presented. We finish the paper with a brief summary and comments on future work in Section 4.

2. Laplace equation

When the flow is irrotational, it is convenient to use velocity potential ϕ as a primary variable, which satisfies the Laplace equation. The no-flow condition on the particle surface corresponds to a Neumann condition on the velocity potential.

2.1. A model problem

Consider the Laplace equation

$$\nabla^2\phi(r,\theta) = 0, \tag{2.1}$$

in $\Omega := \{(r,\theta)|1 < r < R_\infty, 0 \leqslant \theta < 2\pi\}$, subject to Dirichlet conditions

$$\phi(R_\infty,\theta) = \phi_\infty(\theta), \tag{2.2}$$

and

$$\left.\frac{\partial\phi}{\partial r}\right|_{r=1} = 0, \tag{2.3}$$

where ϕ_∞ is a given function of θ. It can be verified that the solution of (2.1) which satisfies (2.3) is

$$\phi(r,\theta) = \sum_{k=1}^{\infty}\left[\alpha_k(r^k + r^{-k})\cos(k\theta) + \beta_k(r^k + r^{-k})\sin(k\theta)\right]. \tag{2.4}$$

And we assume that the coefficients α_k and β_k are chosen such that the far-field condition (2.2) at $r = R_\infty$ is satisfied. We have nondimensionalized r using the particle radius. Thus $r = 1$ represents the particle surface.

We now describe the procedure of PHYSALIS applied to this model problem.

2.2. Procedure of PHYSALIS

Applied to the Laplace equation (2.1) with boundary conditions (2.2) and (2.3), PHYSALIS can be described as an iterative procedure consisting of two steps.

Step 1. At the nth iteration, we solve (2.1) on domain $\Omega/\Omega_1 := \{(r,\theta)|R_1 < r < R_\infty, 0 \leqslant \theta < 2\pi\}$, where $r = R_1$ is the inner cage and R_1 can be greater or less than 1 in which case the cage is inside the cylinder. The far-field solution takes the general form

$$\phi^{(f,n)}(r,\theta) = a_0^{(n)}\log r + \sum_{k=1}^{\infty}\left[(a_k^{(n)}r^k + b_k^{(n)}r^{-k})\cos(k\theta) + (c_k^{(n)}r^k + d_k^{(n)}r^{-k})\sin(k\theta)\right]. \tag{2.5}$$

Here the coefficients $a_k^{(n)}$ and $b_k^{(n)}$ for the kth cosine mode are determined by imposing the far-field condition

$$\phi^{(f,n)}(R_\infty,\theta)=\phi_\infty(\theta), \tag{2.6}$$

and a condition on the inner cage $r=R_1$. This condition is provided by matching $\phi^{(f,n)}$ and $\phi^{(l,n-1)}$, the local solution from the previous iteration, which will be discussed in Step 2. There are various ways to impose this condition and we will discuss in details the Dirichlet condition

$$\phi^{(f,n)}(R_1,\theta)=\phi^{(l,n-1)}(R_1,\theta). \tag{2.7}$$

The coefficients $c_k^{(n)}$ and $d_k^{(n)}$ of the kth sine mode are determined similarly.

Step 2. We solve the Laplace equation on domain $\Omega_2:=\{(r,\theta)|1<r<R_2,0<\theta<2\pi\}$ or $\Omega_2:=\{(r,\theta)|R_2<r<1,0<\theta<2\pi\}$. Here $r=R_2\geqslant R_1$ is the outer cage. The local solution $\phi^{(l,n)}$ takes the form of

$$\phi^{(l,n)}(r,\theta)=\sum_{k=1}^{\infty}\left[\alpha_k^{(n)}(r^k+r^{-k})\cos(k\theta)+\beta_k^{(n)}(r^k+r^{-k})\sin(k\theta)\right]. \tag{2.8}$$

Note that this solution is similar to (2.4) except that the coefficients $\alpha_k^{(n)}$ and $\beta_k^{(n)}$ are different from α_k and β_k since in general the far-field condition (2.2) is not satisfied by $\phi^{(l,n)}$. The values of these coefficients are determined by a boundary condition on the outer cage $r=R_2$, provided by matching $\phi^{(l,n)}$ and $\phi^{(f,n)}$, which is obtained in Step 1. Again, there are several ways to impose the condition and we will study first the Dirichlet condition

$$\phi^{(l,n)}(R_2,\theta)=\phi^{(f,n)}(R_2,\theta). \tag{2.9}$$

Note that neither $\phi^{(f,n)}$ nor $\phi^{(l,n)}$ is the solution of the Laplace equation on the original domain Ω as they only satisfy one of the boundary conditions. However, one can view these two solutions as approximations and more accurate approximations can be obtained by repeating the two steps described above, i.e., when the equation is solved on Ω/Ω_1, one can use $\phi^{(l,n)}$ from the previous iteration to provide the boundary condition on the inner cage and continue the process until convergence is reached.

In practice, one computes the solution $\phi^{(f,n)}$ on Ω/Ω_1 by solving the equations numerically while the solution $\phi^{(l,n)}$ on Ω_2 is represented by the eigenfunction expansion which automatically satisfies the boundary conditions on the particle surface Γ. The coefficients of the eigenfunction expansion is updated using $\phi^{(f,n)}$ during the iterative procedure. In the situations with multiple cylinders, the cages can be set up around each individual cylinder and the numerical solution of the field can be matched up with the analytical expressions around them.

2.3. Convergence analysis

2.3.1. Dirichlet conditions

We first present the results for the Laplace equation using Dirichlet conditions as the matching conditions.

Lemma 2.1. *Let u given by* (2.4) *be the solution of the Laplace equation* (2.1) *on Ω which satisfies* (2.2) *and* (2.3). *Let $\phi^{(f,n)}$ given by* (2.5) *and $\phi^{(l,n)}$ given by* (2.8) *be the far-field and local solution on Ω/Ω_1 and Ω_2, respectively. $\phi^{(f,n)}$ satisfies the far-field condition* (2.2) *and $\phi^{(l,n)}$ satisfies* (2.3). *Then the coefficients of the eigenfunction expansions satisfy the following equations*

$$\alpha_k^{(n)}=\lambda_k\alpha_k^{(n-1)}+(1-\lambda_k)\alpha_k, \tag{2.10}$$

$$\beta_k^{(n)}=\lambda_k\beta_k^{(n-1)}+(1-\lambda_k)\beta_k, \tag{2.11}$$

where

$$\lambda_k = \frac{1-(R_2/R_\infty)^{2k}}{1-(R_1/R_\infty)^{2k}} \frac{R_1^{2k}+1}{R_2^{2k}+1} \tag{2.12}$$

if Dirichlet matching conditions (2.7) *and* (2.9) *are used on both inner and outer cages.*

Proof. In Step 1 of the procedure described earlier, the coefficients $a_k^{(n)}$, $b_k^{(n)}$, $c_k^{(n)}$, and $d_k^{(n)}$ of $\phi^{(f,n)}$ are determined by applying the boundary conditions on $r = R_1$ and $r = R_\infty$. At $r = R_\infty$, we simply use the second condition in (2.2), $\phi^{(f,n)}(R_\infty, \theta) = \phi(R_\infty, \theta)$. And we have

$$\begin{aligned} &a_0^{(n)} = 0, \\ &a_k^{(n)} R_\infty^k + b_k^{(n)} R_\infty^{-k} = \alpha_k (R_\infty^k + R_\infty^{-k}), \\ &c_k^{(n)} R_\infty^k + d_k^{(n)} R_\infty^{-k} = \beta_k (R_\infty^k + R_\infty^{-k}). \end{aligned} \tag{2.13}$$

At $r = R_1$, the solution $\phi^{(f,n)}$ is matched by $\phi^{(l,n-1)}$ using the Dirichlet condition as

$$\begin{aligned} &a_0^{(n)} = 0, \\ &a_k^{(n)} R_1^k + b_k^{(n)} R_1^{-k} = \alpha_k^{(n-1)} (R_1^k + R_1^{-k}), \\ &c_k^{(n)} R_1^k + d_k^{(n)} R_1^{-k} = \beta_k^{(n-1)} (R_1^k + R_1^{-k}). \end{aligned} \tag{2.14}$$

Note that when $n = 1$, we simply assign values for $\alpha_k^{(0)}$ and $\beta_k^{(0)}$ as initial guesses. Using (2.13) and (2.14), the coefficients can be solved as $a_0^{(n)} = 0$ and

$$a_k^{(n)} = -\frac{1}{\Delta_k} R_1^{-k} (R_\infty^k + R_\infty^{-k}) \alpha_k + \frac{1}{\Delta_k} R_\infty^{-k} (R_1^k + R_1^{-k}) \alpha_k^{(n-1)}, \tag{2.15}$$

$$b_k^{(n)} = \frac{1}{\Delta_k} R_1^k (R_\infty^k + R_\infty^{-k}) \alpha_k - \frac{1}{\Delta_k} R_\infty^k (R_1^k + R_1^{-k}) \alpha_k^{(n-1)}, \tag{2.16}$$

$$c_k^{(n)} = -\frac{1}{\Delta_k} R_1^{-k} (R_\infty^k + R_\infty^{-k}) \beta_k + \frac{1}{\Delta_k} R_\infty^{-k} (R_1^k + R_1^{-k}) \beta_k^{(n-1)}, \tag{2.17}$$

$$d_k^{(n)} = \frac{1}{\Delta_k} R_1^k (R_\infty^k + R_\infty^{-k}) \beta_k - \frac{1}{\Delta_k} R_\infty^k (R_1^k + R_1^{-k}) \beta_k^{(n-1)} \tag{2.18}$$

for $k = 1, 2, \ldots,$ where

$$\Delta_k = R_1^k R_\infty^{-k} - R_\infty^k R_1^{-k}.$$

In Step 2 of the procedure, we set up an outer cage $r = R_2 \geqslant R_1$ and match $\phi^{(l,n)}$ at the current (nth) iteration with $\phi^{(f,n)}$ obtained in Step 1, using the Dirichlet condition

$$\phi^{(l,n)}(R_2, \theta) = \phi^{(f,n)}(R_2, \theta).$$

We have

$$\alpha_k^{(n)} = \frac{a_k^{(n)} R_2^k + b_k^{(n)} R_2^{-k}}{R_2^k + R_2^{-k}} = \lambda_k \alpha_k^{(n-1)} + (1-\lambda_k)\alpha_k, \tag{2.19}$$

$$\beta_k^{(n)} = \frac{c_k^{(n)} R_2^k + d_k^{(n)} R_2^{-k}}{R_2^k + R_2^{-k}} = \lambda_k \beta_k^{(n-1)} + (1-\lambda_k)\beta_k \tag{2.20}$$

for $k = 1, 2, \ldots$, where

$$\lambda_k = \frac{1 - (R_2/R_\infty)^{2k}}{1 - (R_1/R_\infty)^{2k}} \frac{R_1^{2k} + 1}{R_2^{2k} + 1}.$$

This concludes the proof. □

The convergence of PHYSALIS for Laplace equation is given by the following corollary and theorem.

Corollary 2.1. *The coefficients $\alpha_k^{(n)}$ and $\beta_k^{(n)}$ of solution $\phi^{(l,n)}$ satisfy the following equation*

$$\begin{pmatrix} \alpha_k^{(n)} \\ \beta_k^{(n)} \end{pmatrix} = \lambda_k^n \begin{pmatrix} \alpha_k^{(0)} \\ \beta_k^{(0)} \end{pmatrix} + (1 - \lambda_k^n) \begin{pmatrix} \alpha_k \\ \beta_k \end{pmatrix}. \tag{2.21}$$

Theorem 2.1. *Let $\phi^{(f,n)}$ (2.5) and $\phi^{(l,n)}$ (2.8) be the far-field and local solutions of the Laplace equation generated by the iterative procedure PHYSALIS. Then they converge to the exact solution u (2.4) if and only if $\lambda_k < 1$ for all nonnegative integers k.*

Proof. Since $\lambda_k < 1$, we have $\lim_{n\to\infty} \lambda_k^n = 0$. Using Corollary 2.1, we have $\alpha_k^{(n)} \to \alpha_k$, $\beta_k^{(n)} \to \beta_k$, Thus solution (2.5) converges to (2.4). From (2.15), we have

$$\begin{aligned} \lim_{n\to\infty} a_k^{(n)} &= \lim_{n\to\infty} \left\{ -\frac{1}{\Delta_k} R_1^{-k} (R_\infty^k + R_\infty^{-k})\alpha_k + \frac{1}{\Delta_k} R_\infty^{-k} (R_1^k + R_1^{-k}) \alpha_k^{(n)} \right\} \\ &= -\frac{1}{\Delta_k} R_1^{-k} (R_\infty^k + R_\infty^{-k})\alpha_k + \frac{1}{\Delta_k} R_\infty^{-k} (R_1^k + R_1^{-k})\alpha_k = \frac{1}{\Delta_k} \{R_\infty^{-k} R_1^k - R_1^{-k} R_\infty^k\}\alpha_k = \alpha_k. \end{aligned}$$

Similarly, from (2.16)–(2.18), we can show that

$$b_k^{(n)} \to -\alpha_k, c_k^{(n)} \to \beta_k, d_k^{(n)} \to -\beta_k.$$

Thus the solution $\phi^{(f,n)}$ given by (2.8) also converges to the solution u given by (2.4). This concludes the proof of the theorem. □

2.3.2. Other conditions

When the Laplace equation (2.1) is solved on Ω subject to (2.2) and (2.3), other matching condition such as a Neumann condition can be used on both cages, i.e.,

$$\frac{\partial}{\partial r} \phi^{(f,n)}(R_1, \theta) = \frac{\partial}{\partial r} \phi^{(l,n-1)}(R_1, \theta), \tag{2.22}$$

$$\frac{\partial}{\partial r} \phi^{(l,n)}(R_2, \theta) = \frac{\partial}{\partial r} \phi^{(f,n)}(R_2, \theta). \tag{2.23}$$

Or a combination of Dirichlet and Neumann conditions on inner and outer cages can also be used. It is not difficulty to show that the coefficients of the eigenfunction expansion $\alpha_k^{(n)}$, $\beta_k^{(n)}$, α_k, and β_k satisfy the same recurrence formula (2.10) and (2.11) where

$$\lambda_k = \frac{1 + (R_2/R_\infty)^{2k}}{1 - (R_1/R_\infty)^{2k}} \frac{R_1^{2k} + 1}{R_2^{2k} - 1}, \tag{2.24}$$

using (2.7) and (2.23),

$$\lambda_k = \frac{1 - (R_2/R_\infty)^{2k}}{1 + (R_1/R_\infty)^{2k}} \frac{R_1^{2k} - 1}{R_2^{2k} + 1}, \tag{2.25}$$

using (2.22) and (2.9), and finally

$$\lambda_k = \frac{1 + (R_2/R_\infty)^{2k}}{1 + (R_1/R_\infty)^{2k}} \frac{R_1^{2k} - 1}{R_2^{2k} - 1}, \tag{2.26}$$

using (2.22) and (2.23).

Obviously Corollary 2.1 and Theorem 2.1 are applicable to these matching conditions. Therefore, the convergence of PHYSALIS using different boundary and matching conditions depends on the values of λ_k given above, which are discussed next.

2.3.3. Discussion

In general, the absolute value of λ_k given by (2.25) is the smallest, followed by (2.12), (2.26), and (2.24). Therefore the Neumann condition is preferred on the outer cage and should be avoided on the inner cage. In particular, we can make the following observations.

When Dirichlet matching conditions (2.7) and (2.9) are used on both inner and outer cages, in order for the method to converge, we need to have $\lambda_k < 1$ where

$$\lambda_k = \frac{1 - (R_2/R_\infty)^{2k}}{1 - (R_1/R_\infty)^{2k}} \frac{R_1^{2k} + 1}{R_2^{2k} + 1}.$$

It is clear that $0 \leqslant \lambda_k < 1$ as long as $R_1 < R_2$. Thus the method converges regardless of the values of R_1, R_2 and k. Furthermore, for fixed values of R_1 and R_2 with $1 \leqslant R_1 < R_2$, $\lambda_k \to (R_1/R_2)^{2k}$ as $k \to \infty$, which indicates that convergence is asymptotically faster for higher modes. On the other hand, if $R_1 < R_2 \leqslant 1$, $\lambda_k \to 1$ as $k \to \infty$, which indicates that convergence is asymptotically slower for higher modes. It can also be observed that the method does not converge when only one cage is used since $\lambda_k = 1$ when $R_2 = R_1$.

When Dirichlet matching condition (2.9) is used on the outer cage and Neumann matching condition (2.22) is used on the inner cage, we have

$$\lambda_k = \frac{1 - (R_2/R_\infty)^{2k}}{1 + (R_1/R_\infty)^{2k}} \frac{R_1^{2k} - 1}{R_2^{2k} + 1}.$$

Obviously, $\lambda_k < 1$ for any choices of R_1 and R_2 including the case of $R_1 = R_2$ (single cage approach) and the case of $R_1, R_2 < 1$ (cages inside the cylinder). Furthermore, $\lambda_k \to \max\{1, R_1^{2k}\}/\max\{R_2^{2k}, 1\}$ as $k \to \infty$. Thus, if $R_1, R_2 < 1$, then $\lambda_k \to 1$ as $k \to \infty$, which indicates that convergence slows down for high-order modes if the cages are both placed inside the cylinder. Finally, the eigenvalues of this case is always smaller than those in the previous case, indicating that convergence is faster.

For the remaining two cases, the convergence of the iteration is not guaranteed, indicated by (2.24) and (2.26). Therefore, these matching conditions should be avoided in practice. We now turn our attention to the biharmonic equation.

3. Biharmonic equation

In the case of large viscosity or more accurately of small Reynolds numbers, Stokes flows are often used as an approximation, where the stream-function satisfies the biharmonic equation. Biharmonic equation also arises in other areas such as the linear elasticity theory. But we will focus on the fluid flows.

3.1. A model problem

Consider the biharmonic equation for ψ

$$\nabla^2\nabla^2\psi(r,\theta) = 0, \tag{3.1}$$

in $\Omega := \{(r,\theta)|1 < r < R_\infty, 0 \leqslant \theta < 2\pi\}$, subject to boundary conditions

$$\psi = \frac{\partial\psi}{\partial r} = 0, \quad \text{when } r = 1, \tag{3.2}$$

and

$$\psi = \psi_\infty, \quad \frac{\partial\psi}{\partial r} = u_\infty, \quad \text{when } r = R_\infty, \tag{3.3}$$

where ψ_∞ and u_∞ are given function of θ. Boundary condition (3.2) is called the no-slip condition, in the context of Stokes flows, when the particle velocity is zero.

It is easy to verify that the solution of (3.1) which satisfies the no-slip condition (3.2) is [1]

$$\begin{aligned}\psi(r,\theta) = {} & \alpha_0\left(r^2 - 2\log r - 1\right) + \left[\alpha_1(r^3 - 2r + r^{-1}) + \beta_1(r\log r - r/2 + r^{-1}/2)\right]\cos(\theta) \\ & + \left[\hat{\alpha}_1(r^3 - 2r + r^{-1}) + \hat{\beta}_1(r\log r - r/2 + r^{-1}/2)\right]\sin(\theta) + \sum_{k=2}^{\infty}\left[\alpha_k(kr^{k+2} - (k+1)r^k + r^{-k})\right. \\ & \left. + \beta_k(kr^{2-k} - (k-1)r^{-k} - r^k)\right]\cos(k\theta) + \sum_{k=2}^{\infty}\left[\hat{\alpha}_k(kr^{k+2} - (k+1)r^k + r^{-k})\right. \\ & \left. + \hat{\beta}_k(kr^{2-k} - (k-1)r^{-k} - r^k)\right]\sin(k\theta).\end{aligned} \tag{3.4}$$

For each cosine (sine) mode, there are two coefficients α_k and β_k ($\hat{\alpha}_k$ and $\hat{\beta}_k$) to be determined by the far-field condition (3.3).

3.2. Procedure of PHYSALIS

Similar to our discussion for the Laplace equation, the procedure of PHYSALIS, when it is applied to the biharmonic equation (3.1), can be described by the following two steps.

Step 1. We solve (3.1) on domain $\Omega/\Omega_1 := \{(r,\theta)|R_1 < r < R_\infty, 0 \leqslant \theta < 2\pi\}$, where $r = R_1$ is the inner cage. The far-field solution $\psi^{(f,n)}$ takes the general form of [2]

[1] It can be shown that at the zeroth order $\beta_0(r^2 - 1)\log r$ must vanish otherwise the pressure will not be periodic in the θ direction.

[2] The term $b_0^{(n)} r^2 \log r$ is not present since the pressure will not be periodic in the θ direction otherwise.

$$\psi^{(f,n)}(r,\theta) = a_0^{(n)} r^2 + c_0^{(n)} \log r + d_0^{(n)} + \left(a_1^{(n)} r^3 + b_1^{(n)} r \log r + c_1^{(n)} r + d_1^{(n)} r^{-1}\right) \cos(\theta) + \left(\hat{a}_1^{(n)} r^3 + \hat{b}_1^{(n)} r \log r + \hat{c}_1^{(n)} r + \hat{d}_1^{(n)} r^{-1}\right) \sin(\theta) + \sum_{k=2}^{\infty} \left(a_k^{(n)} r^{k+2} + b_k^{(n)} r^{2-k} + c_k^{(n)} r^k + d_k^{(n)} r^{-k}\right) \times \cos(k\theta) + \sum_{k=2}^{\infty} \left(\hat{a}_k^{(n)} r^{k+2} + \hat{b}_k^{(n)} r^{2-k} + \hat{c}_k^{(n)} r^k + \hat{d}_k^{(n)} r^{-k}\right) \sin(k\theta), \tag{3.5}$$

where the superscript n denotes the solution at the nth iteration. For each cosine and sine modes in the expansion, there are four constant coefficients, which can be determined as follows. Since the coefficients for the sine modes can be determined in the same way as the cosine modes, we will not discuss them explicitly in the rest of the paper. First we obtain two equations for four coefficients $a_k^{(n)}$, $b_k^{(n)}$, $c_k^{(n)}$, and $d_k^{(n)}$ in the kth cosine mode by imposing the far-field condition

$$\psi^{(f,n)} = \psi_\infty(\theta), \quad \frac{\partial \psi^{(f,n)}}{\partial r} = u_\infty(\theta), \quad r = R_\infty. \tag{3.6}$$

The other two equations are provided by matching $\psi^{(f,n)}$ with $\psi^{(l,n-1)}$), the local solution from the previous iteration $n-1$, which will be discussed in Step 2. There are various ways to impose the matching conditions and in this paper we will discuss two approaches. The simplest is to match the velocity

$$\frac{\partial \psi^{(f,n)}}{\partial \theta} = \frac{\partial \psi^{(l,n-1)}}{\partial \theta}, \quad \frac{\partial \psi^{(f,n)}}{\partial r} = \frac{\partial \psi^{(l,n-1)}}{\partial r}, \quad r = R_1. \tag{3.7}$$

Step 2. We solve the biharmonic equation on domain $\Omega_2 := \{(r,\theta)|1 < r < R_2, 0 < \theta < 2\pi\}$ or $\Omega_2 := \{(r,\theta)|R_2 < r < 1, 0 < \theta < 2\pi\}$, where $r = R_2 \geqslant R_1$ is the outer cage. We impose the no-slip condition (3.2) and the local solution $\psi^{(l,n)}$ can be written as

$$\begin{aligned}\psi^{(l,n)}(r,\theta) = {} & \alpha_0^{(n)}\left(r^2 - 2\log r - 1\right) + \left[\alpha_1^{(n)}(r^3 - 2r + r^{-1}) + \beta_1^{(n)}(r\log r - r/2 + r^{-1}/2)\right]\cos(\theta) \\ & + \left[\hat{\alpha}_1^{(n)}(r^3 - 2r + r^{-1}) + \hat{\beta}_1^{(n)}(r\log r - r/2 + r^{-1}/2)\right]\sin(\theta) \\ & + \sum_{k=2}^{\infty}\left[\alpha_k^{(n)}(kr^{k+2} - (k+1)r^k + r^{-k}) + \beta_k^{(n)}(kr^{2-k} - (k-1)r^{-k} - r^k)\right]\cos(k\theta) \\ & + \sum_{k=2}^{\infty}\left[\hat{\alpha}_k^{(n)}(kr^{k+2} - (k+1)r^k + r^{-k}) + \hat{\beta}_k^{(n)}(kr^{2-k} - (k-1)r^{-k} - r^k)\right]\sin(k\theta).\end{aligned} \tag{3.8}$$

Note that this solution is similar to (3.4) except that the coefficients α_k and β_k are replaced by $\alpha_k^{(n)}$ and $\beta_k^{(n)}$. In general $\alpha_k^{(n)}$ and $\beta_k^{(n)}$ are different from α_k and β_k since the far-field condition in (3.3) is not satisfied by $\psi^{(l,n)}$. The values of these coefficients are determined by 'boundary conditions' on the outer cage $r = R_2$, which is provided by matching $\psi^{(l,n)}$ with $\psi^{(f,n)}$ obtained in Step 1. Again, there are several approaches can be used and one of these is to match the velocity

$$\frac{\partial \psi^{(l,n)}}{\partial \theta} = \frac{\partial \psi^{(f,n)}}{\partial \theta}, \quad \frac{\partial \psi^{(l,n)}}{\partial r} = \frac{\partial \psi^{(f,n)}}{\partial r}, \quad r = R_2. \tag{3.9}$$

Other approaches can also be used. For example, one can match vorticity and pressure and the details of this matching condition will be discussed in Section 3.3.2.

3.3. Convergence analysis

We first present the main convergence results when the velocity is matched on both the inner and outer cages.

3.3.1. Velocity matching conditions

Lemma 3.1. *Let ψ given in* (3.4) *be the solution of the biharmonic equation* (3.1) *on Ω which satisfies both* (3.2) *and* (3.3). *Let $\psi^{(f,n)}$ given by* (3.5) *and $\psi^{(l,n)}$ given by* (3.8) *be the far-field and local solutions on Ω/Ω_1 and Ω_2, respectively. $\psi^{(f,n)}$ satisfies the far-field condition* (3.3) *and $\psi^{(l,n)}$ satisfies the no-slip condition* (3.2). *Velocity conditions* (3.7) *and* (3.9) *are used on inner cage to match $\psi^{(f,n)}$ and $\psi^{(l,n-1)}$ and on outer cage to match $\psi^{(f,n)}$ and $\psi^{(l,n)}$. Then the coefficients of the eigenfunction expansions satisfy the following equations*

$$\alpha_0^{(n)} = \rho_0\alpha_0^{(n-1)} + (1-\rho_0)\alpha_0, \quad \hat{\alpha}_0^{(n)} = \rho_0\hat{\alpha}_0^{(n-1)} + (1-\rho_0)\hat{\alpha}_0, \tag{3.10}$$

where

$$\rho_0 = \frac{(R_\infty^2 - R_2^2)(R_1^2 - 1)}{(R_\infty^2 - R_1^2)(R_2^2 - 1)}.$$

For $k \geqslant 1$,

$$\begin{pmatrix} \alpha_k^{(n)} \\ \beta_k^{(n)} \end{pmatrix} = T_k \begin{pmatrix} \alpha_k^{(n-1)} \\ \beta_k^{(n-1)} \end{pmatrix} + (I - T_k)\begin{pmatrix} \alpha_k \\ \beta_k \end{pmatrix}, \tag{3.11}$$

$$\begin{pmatrix} \hat{\alpha}_k^{(n)} \\ \hat{\beta}_k^{(n)} \end{pmatrix} = T_k \begin{pmatrix} \hat{\alpha}_k^{(n-1)} \\ \hat{\beta}_k^{(n-1)} \end{pmatrix} + (I - T_k)\begin{pmatrix} \hat{\alpha}_k \\ \hat{\beta}_k \end{pmatrix}, \tag{3.12}$$

where T_k is a 2×2 square matrix given by

$$T_k = D_k^{-1}E_kA_k^{-1}\begin{pmatrix} B_k \\ 0 \end{pmatrix},$$

and

$$A_k = \begin{pmatrix} R_1^{k+2} & R_1^{2-k} & R_1^k & R_1^{-k} \\ (k+2)R_1^{k+2} & (2-k)R_1^{2-k} & kR_1^k & -kR_1^{-k} \\ R_\infty^{k+2} & R_\infty^{2-k} & R_\infty^k & R_\infty^{-k} \\ (k+2)R_\infty^{k+2} & (2-k)R_\infty^{2-k} & kR_\infty^k & -kR_\infty^{-k} \end{pmatrix}, \tag{3.13}$$

$$B_k = \begin{pmatrix} kR_1^{k+2} - (k+1)R_1^k + R_1^{-k} & kR_1^{2-k} - (k-1)R_1^{-k} - R_1^k \\ k(k+2)R_1^{k+2} - (k+1)kR_1^{2-k} - kR_1^{-k} & k(2-k)R_1^{2-k} + k(k-1)R_1^{-k} - kR_1^k \end{pmatrix}, \tag{3.14}$$

$$D_k = \begin{pmatrix} kR_2^{k+2} - (k+1)R_2^k + R_2^{-k} & kR_2^{2-k} - (k-1)R_2^{-k} - R_2^k \\ k(k+2)R_2^{k+2} - (k+1)kR_2^{2-k} - kR_2^{-k} & k(2-k)R_2^{2-k} + k(k-1)R_2^{-k} - kR_2^k \end{pmatrix}, \tag{3.15}$$

$$E_k = \begin{pmatrix} R_2^{k+2} & R_2^{2-k} & R_2^k & R_2^{-k} \\ (k+2)R_2^{k+2} & (2-k)R_2^{2-k} & kR_2^k & -kR_2^{-k} \end{pmatrix} \tag{3.16}$$

for $k \geqslant 2$, and when $k = 1$,

$$A_1 = \begin{pmatrix} R_1^3 & R_1 \log R_1 & R_1 & R_1^{-1} \\ 3R_1^3 & R_1(\log R_1 + 1) & R_1 & -R_1^{-1} \\ R_\infty^3 & R_\infty \log R_\infty & R_\infty & R_\infty^{-1} \\ 3R_\infty^3 & R_\infty(\log R_\infty + 1) & R_\infty & -R_\infty^{-1} \end{pmatrix}, \tag{3.17}$$

$$B_1 = \begin{pmatrix} R_1^3 - 2R_1 + R_1^{-1} & R_1 \log R_1 - R_1/2 + R_1^{-1}/2 \\ 3R_1^3 - 2R_1 - R_1^{-1} & R_1 \log R_1 + R_1/2 - R_1^{-1}/2 \end{pmatrix}, \tag{3.18}$$

$$D_1 = \begin{pmatrix} R_2^3 - 2R_2 + R_2^{-1} & R_2 \log R_2 - R_2/2 + R_2^{-1}/2 \\ 3R_2^3 - 2R_2 - R_2^{-1} & R_2 \log R_2 + R_2/2 - R_2^{-1}/2 \end{pmatrix}, \tag{3.19}$$

$$E_1 = \begin{pmatrix} R_2^3 & R_2 \log R_2 & R_2 & R_2^{-1} \\ 3R_2^3 & R_2(\log R_2 + 1) & R_2 & -R_2^{-1} \end{pmatrix}. \tag{3.20}$$

Proof. To prove this lemma, we simply go through the two steps described earlier. Since the discussion is similar for $k = 0$, $k = 1$, and for $k \geqslant 2$, we only provide the details for $k \geqslant 2$. In Step 1 of the procedure described previously, to determine the coefficients $a_k^{(n)}$, $b_k^{(n)}$, $c_k^{(n)}$, and $d_k^{(n)}$ of $\psi^{(f,n)}$, we apply the far-field condition (3.3) which yields two equations for $k \geqslant 2$

$$R_\infty^{k+2} a_k^{(n)} + R_\infty^{2-k} b_k^{(n)} + R_\infty^k c_k^{(n)} + R_\infty^{-k} d_k^{(n)} = (kR_\infty^{2+k} - (k+1)R_\infty^k + R_\infty^{-k})\alpha_k + (kR_\infty^{2-k} - (k-1)R_\infty^{-k} - R_\infty^k)\beta_k, \tag{3.21}$$

$$\begin{aligned} &(k+2)R_\infty^{k+2} a_k^{(n)} + (2-k)R_\infty^{2-k} b_k^{(n)} + kR_\infty^k c_k^{(n)} - kR_\infty^{-k} d_k^{(n)} \\ &\quad = (k(k+2)R_\infty^{2+k} - k(k+1)R_\infty^k - kR_\infty^{-k})\alpha_k + (k(2-k)R_\infty^{2-k} + k(k-1)R_\infty^{-k} - kR_\infty^k)\beta_k. \end{aligned} \tag{3.22}$$

Assuming that the solution $\psi^{(l,n-1)}$ from the previous iteration (denoted by the superscript $n-1$) is known, the matching condition (3.7) provides another two equations for $k \geqslant 2$

$$R_1^{k+2} a_k^{(n)} + R_1^{2-k} b_k^{(n)} + R_1^k c_k^{(n)} + R_1^{-k} d_k^{(n)} = \left[kR_1^{2+k} - (k+1)R_1^k + R_1^{-k}\right]\alpha_k^{(n-1)} + \left[kR_1^{2-k} - (k-1)R_1^{-k} - R_1^k\right]\beta_k^{(n-1)}, \tag{3.23}$$

$$\begin{aligned} &(k+2)R_1^{k+2} a_k^{(n)} + (2-k)R_1^{2-k} b_k^{(n)} + kR_1^k c_k^{(n)} - kR_1^{-k} d_k^{(n)} \\ &\quad = k\left[(k+2)R_1^{2+k} - (k+1)R_1^k - R_1^{-k}\right]\alpha_k^{(n-1)} + k\left[(2-k)R_1^{2-k} + (k-1)R_1^{-k} - R_1^k\right]\beta_k^{(n-1)}. \end{aligned} \tag{3.24}$$

Combining these four equations we have the matrix form

$$A_k \begin{pmatrix} a_k^{(n)} \\ b_k^{(n)} \\ c_k^{(n)} \\ d_k^{(n)} \end{pmatrix} = \begin{pmatrix} B_k & 0 \\ 0 & C_k \end{pmatrix} \begin{pmatrix} \alpha_k^{(n-1)} \\ \beta_k^{(n-1)} \\ \alpha_k \\ \beta_k \end{pmatrix}, \tag{3.25}$$

where A_k and B_k are given by (3.13) and (3.14), and

$$C_k = \begin{pmatrix} kR_\infty^{k+2} - (k+1)R_\infty^{k} + R_\infty^{-k} & kR_\infty^{2-k} - (k-1)R_\infty^{-k} - R_\infty^{k} \\ k(k+2)R_\infty^{k+2} - (k+1)kR_\infty^{k} - kR_\infty^{-k} & k(2-k)R_\infty^{2-k} + k(k-1)R_\infty^{-k} - kR_\infty^{k} \end{pmatrix}. \tag{3.26}$$

From Step 2 of the procedure, we have the solution $\psi^{(l,n)}$ of the form (3.8) with coefficients $\alpha_k^{(n)}$ and $\beta_k^{(n)}$ to be determined by matching condition (3.9), which yields

$$\begin{aligned} &\left[kR_2^{2+k} - (k+1)R_2^{k} + R_2^{-k}\right]\alpha_k^{(n)} + \left[kR_2^{2-k} - (k-1)R_2^{-k} - R_2^{-k}\right]\beta_k^{(n)} \\ &\quad = R_2^{k+2}a_k^{(n)} + R_2^{2-k}b_k^{(n)} + R_2^{k}c_k^{(n)} + R_2^{-k}d_k^{(n)}, \end{aligned} \tag{3.27}$$

$$\begin{aligned} &k\left[(k+2)R_2^{2+k} - (k+1)R_2^{k} - R_2^{-k}\right]\alpha_k^{(n)} + k\left[(2-k)R_2^{2-k} + (k-1)R_2^{-k} + R_2^{-k}\right]\beta_k^{(n)} \\ &\quad = (k+2)R_2^{k+2}a_k^{(n)} + (2-k)R_2^{2-k}b_k^{(n)} + kR_2^{k}c_k^{(n)} - kR_2^{-k}d_k^{(n)}, \end{aligned} \tag{3.28}$$

which can be written into a short matrix form as

$$D_k \begin{pmatrix} \alpha_k^{(n)} \\ \beta_k^{(n)} \end{pmatrix} = E_k \begin{pmatrix} a_k^{(n)} \\ b_k^{(n)} \\ c_k^{(n)} \\ d_k^{(n)} \end{pmatrix}, \tag{3.29}$$

where D_k and E_k are given by (3.15) and (3.16). From (3.25) and (3.29), we obtain

$$\begin{pmatrix} \alpha_k^{(n)} \\ \beta_k^{(n)} \end{pmatrix} = D_k^{-1}E_kA_k^{-1}\begin{pmatrix} B_k \\ 0 \end{pmatrix}\begin{pmatrix} \alpha_k^{(n-1)} \\ \beta_k^{(n-1)} \end{pmatrix} + D_k^{-1}E_kA_k^{-1}\begin{pmatrix} 0 \\ C_k \end{pmatrix}\begin{pmatrix} \alpha_k \\ \beta_k \end{pmatrix}.$$

After some algebraic manipulations, one can show that

$$D_k^{-1}E_kA_k^{-1}\begin{pmatrix} B_k \\ C_k \end{pmatrix} = I.$$

Note that

$$T_k = D_k^{-1}E_kA_k^{-1}\begin{pmatrix} B_k \\ 0 \end{pmatrix},$$

(3.11) follows immediately and (3.12) can be derived similarly. Similar derivation can be carried out for $k = 0$ and 1, therefore we conclude the proof of the lemma. □

The convergence of PHYSALIS using velocity matching conditions (3.7) and (3.9) is given by the following corollaries and theorem.

Corollary 3.1. *The coefficients $\alpha_k^{(n)}$ and $\beta_k^{(n)}$ of the local solution $\psi^{(l,n)}$ satisfy the following equations*

$$\alpha_0^{(n)} = (\rho_0)^n\left(\alpha_0^{(n-1)} - \alpha_0\right) + \alpha_0, \tag{3.30}$$

$$\begin{pmatrix} \alpha_k^{(n)} \\ \beta_k^{(n)} \end{pmatrix} = (T_k)^n\begin{pmatrix} \alpha_k^{(n-1)} - \alpha_k \\ \beta_k^{(n-1)} - \beta_k \end{pmatrix} + \begin{pmatrix} \alpha_k \\ \beta_k \end{pmatrix}, \quad k \geqslant 1. \tag{3.31}$$

Corollary 3.2. *The coefficients $\hat{\alpha}_k^{(n)}$ and $\hat{\beta}_k^{(n)}$ of solution $\psi^{(l,n)}$ satisfy the following equations*

$$\hat{\alpha}_0^{(n)} = (\rho_0)^n\left(\hat{\alpha}_0^{(n-1)} - \hat{\alpha}_0\right) + \hat{\alpha}_0, \tag{3.32}$$

$$\begin{pmatrix} \hat{\alpha}_k^{(n)} \\ \hat{\beta}_k^{(n)} \end{pmatrix} = (T_k)^n \begin{pmatrix} \hat{\alpha}_k^{(n-1)} - \hat{\alpha}_k \\ \hat{\beta}_k^{(n-1)} - \hat{\beta}_k \end{pmatrix} + \begin{pmatrix} \hat{\alpha}_k \\ \hat{\beta}_k \end{pmatrix}, \quad k \geqslant 1. \tag{3.33}$$

Theorem 3.1. *Let $\psi^{(f,n)}$ and $\psi^{(l,n)}$ be the far-field and local solutions of the biharmonic equation generated by the iterative procedure PHYSALIS. Then they converge to the exact solution ψ if and only if $\rho_0 < 1$ and $\rho_k < 1$ for all positive integer k, where ρ_k is the spectral radius of matrix T_k.*

Proof. Since $\rho_k < 1$, we have $\lim_{n\to\infty} T_k^n = 0$. Using Corollary 3.1 and 3.2, we have $\alpha_k^{(n)} \to \alpha_k$, $\beta_k^{(n)} \to \beta_k$, $\hat{\alpha}_k^{(n)} \to \hat{\alpha}_k$ and $\hat{\beta}_k^{(n)} \to \hat{\beta}_k$ for $k = 0, 1, 2, \ldots$ Thus solution $\psi^{(l,n)}$ given by (3.8) converges to ψ given by (3.4). Since the solution of the biharmonic equation with the given boundary conditions are unique, we conclude that solution $\psi^{(f,n)}$ given by (3.5) also converges to ψ given by (3.4). This concludes the proof of the theorem. □

Even though Lemma 3.1 is proved for PHYSALIS using particular matching conditions (3.7) and (3.9), it it not difficult to see that other matching conditions will lead to similar conclusions, which will be discussed briefly next.

3.3.2. Other matching conditions

The main reason for using other matching conditions is that the velocity matching condition does not work for a single cage approach (see Section 3.3.3). Furthermore, the Stokes approximation may only be valid in the boundary layer outside the cylinder. Therefore, it is desirable to put cages inside the cylinder, for which the method does not converge using the velocity matching condition (Section 3.3.3). In this paper, we analyze another approach which uses velocity condition on the inner cage $r = R_1$ and match the pressure and vorticity on the outer cage $r = R_2$. This is a natural approach since both pressure and vorticity are primary variables.

Since the first step for this approach is identical to that of velocity matching, we only need to find the matching equations for the second step. It is not difficult to verify that the pressure and vorticity can be obtained as

$$\begin{aligned} p^{(f,n)}(r,\theta) = p_0^{(f,n)} &+ 2\left(4a_1^{(n)} r - b_1^{(n)} r^{-1}\right)\cos(\theta) - 2\left(4\hat{a}_1^{(n)} r - \hat{b}_1^{(n)} r^{-1}\right)\sin(\theta) + 4\sum_k \left[a_k^{(n)}(k+1)r^k \right. \\ &\left. - b_k^{(n)}(1-k)r^{-k}\right]\cos(k\theta) - 4\sum_k \left[\hat{a}_k^{(n)}(k+1)r^k - \hat{b}_k^{(n)}(1-k)r^{-k}\right]\sin(k\theta), \end{aligned} \tag{3.34}$$

$$\begin{aligned} \omega^{(f,n)}(r,\theta) = -4a_0^{(n)} &- 2\left(4a_1^{(n)} r + b_1^{(n)} r^{-1}\right)\cos(\theta) - 2\left(4\hat{a}_1^{(n)} r + \hat{b}_1^{(n)} r^{-1}\right)\sin(\theta) - 4\sum_k \left[a_k^{(n)}(k+1)r^k \right. \\ &\left. + b_k^{(n)}(1-k)r^{-k}\right]\cos(k\theta) - 4\sum_k \left[\hat{a}_k^{(n)}(k+1)r^k + \hat{b}_k^{(n)}(1-k)r^{-k}\right]\sin(k\theta) \end{aligned} \tag{3.35}$$

corresponding to the solution $\psi^{(f,n)}$. For $\psi^{(l,n)}$, we have

$$p^{(l,n)}(r,\theta) = p_0^{(l,n)} + 2\left(4\alpha_1^{(n)} r - \beta_1^{(n)} r^{-1}\right)\cos(\theta) - 2\left(4\hat{\alpha}_1^{(n)} r - \hat{\beta}_1^{(n)} r^{-1}\right)\sin(\theta) + 4\sum_k \left[\alpha_k^{(n)}(k+1)kr^k - \beta_k^{(n)}(1-k)kr^{-k}\right]\cos(k\theta) - 4\sum_k \left[\hat{\alpha}_k^{(n)}(k+1)kr^k - \hat{\beta}_k^{(n)}(1-k)kr^{-k}\right]\sin(k\theta), \tag{3.36}$$

$$\omega^{(l,n)}(r,\theta) = -4\alpha_0^{(n)} - 2\left(4\alpha_1^{(n)} r + \beta_1^{(n)} r^{-1}\right)\cos(\theta) - 2\left(4\hat{\alpha}_1^{(n)} r + \hat{\beta}_1^{(n)} r^{-1}\right)\sin(\theta) - 4\sum_k \left[\alpha_k^{(n)}(k+1)kr^k + \beta_k^{(n)}(1-k)kr^{-k}\right]\cos(k\theta) - 4\sum_k \left[\hat{\alpha}_k^{(n)}(k+1)kr^k + \hat{\beta}_k^{(n)}(1-k)kr^{-k}\right]\sin(k\theta). \tag{3.37}$$

When the pressure and vorticity values are matched on the outer cage, i.e.,

$$p^{(l,n)}(R_2,\theta) = p^{(f,n)}(R_2,\theta), \quad \omega^{(l,n)}(R_2,\theta) = \omega^{(f,n)}(R_2,\theta), \tag{3.38}$$

we have $p_0^{(f,n)} = p_0^{(l,n)}$, and for higher order cosine modes

$$D_k \begin{pmatrix} \alpha_k^{(n)} \\ \beta_k^{(n)} \end{pmatrix} = E_k \begin{pmatrix} a_k^{(n)} \\ b_k^{(n)} \end{pmatrix}, \tag{3.39}$$

where

$$D_k = \begin{pmatrix} (k+1)R_2^k & -(1-k)R_2^{-k} \\ (k+1)R_2^k & (k-1)R_2^{-k} \end{pmatrix}, \tag{3.40}$$

$$E_k = \begin{pmatrix} kD_k & 0 \end{pmatrix} \tag{3.41}$$

for $k \geqslant 2$. And for $k = 1$, we have

$$D_1 = \begin{pmatrix} 4R_2 & -R_2^{-1} \\ 4R_2 & R_2^{-1} \end{pmatrix}, \tag{3.42}$$

$$E_1 = \begin{pmatrix} D_1 & 0 \end{pmatrix}. \tag{3.43}$$

The iterative matrix is

$$T_k = (D_k)^{-1} E_k A_k^{-1} \begin{pmatrix} B_k \\ 0 \end{pmatrix},$$

where A_k and B_k are given earlier in (3.13) and (3.14). For $k = 0$, we simply have $\alpha_0^{(n)} = a_0^{(n)} = \alpha_0$. The derivation for the coefficients of the sine modes is identical.

3.3.3. Discussion

As we have shown previously, the convergence of PHYSALIS for biharmonic equation depends on whether ρ_0 and the spectral radius of the iterative matrix T_k are less than one. We first consider the case when velocity matching conditions are used. For $k = 0$ (the zeroth mode), the convergence rate depends on

$$\rho_0 = \frac{1 - (R_2/R_\infty)^2}{1 - (R_1/R_\infty)^2} \frac{R_1^2 - 1}{R_2^2 - 1}.$$

It can be seen clearly that $0 \leqslant \rho_0 < 1$ as long as $1 \leqslant R_1 < R_2 \leqslant R_\infty$. On the other hand, we may have $\rho_0 > 1$ when $R_1 < R_2 < 1$. Furthermore, $\rho_0 = 1$ when $R_2 = R_1$. This indicates that the iteration may not converge for a single cage case or if the cages are inside the cylinder. When the two cages are both outside the cylinder, the zeroth mode converges. Whether the method converges or not will depend on the higher order modes, i.e., when $k \geqslant 1$.

For the modes with $k \geqslant 1$, even though the analytical expression of the eigenvalues of T_k can be obtained, they are too complicated to be useful. Instead, we computed the spectral radius numerically using Matlab. As shown in Fig. 2, the spectral radius ρ_k of T_k is less than one for all k (up to $k = 10$ for our computation) when $1 \leqslant R_1 < R_2 \leqslant R_\infty$. The largest value occurs when $k = 1$ which indicates that the convergence is the slowest for this mode. As long as R_2 is not too close to R_1, the spectral radius of T_k is much smaller than one. Therefore, the method will converge and a reasonable rate for all the coefficients in the eigenfunction expansion, thus the flow fields.

When the pressure and vorticity are used in the matching conditions to update the coefficients in the eigenfunction expansion, we note that the convergence for the $k = 0$ mode is achieved in one iteration. Furthermore, since $D_k^{-1}E_k = (kI\ 0)$, the iterative matrix T_k is independent of R_2. This means that the location of outer cage is irrelevant for the convergence of the method. An obvious choice for the outer cage is therefore the inner cage and the computation can be carried out on a single cage. In Fig. 3, the spectral radius ρ_k is plotted as a function of R_1 the inner (single) cage radius and k. It can be seen that the method is convergent since $\rho_k < 1$ when $0 < R_1 < 1$ and $1 \leqslant k \leqslant 10$. However, it can be also observed that $\rho_k \to 1$ as $k \to \infty$ or $R_1 \to 0$. Thus, convergence becomes slow for high frequency modes or when the cage radius is small. In practice, one usually truncate the eigenfunction expansion. Thus, in order to achieve reasonable convergence rate, one should place the cage as close to the cylinder surface as possible, as indicated by Fig. 3.

When $R_1 > 1$, i.e., the cage is located outside the cylinder, the spectral radius ρ_k is plotted in Fig. 4. It can be seen clearly that ρ_k increases rapidly from zero (when $R_1 = 1$) to some large value (greater than one for most of the k plotted) as R_1 increases. Even though one can in principle always locate the inner cage

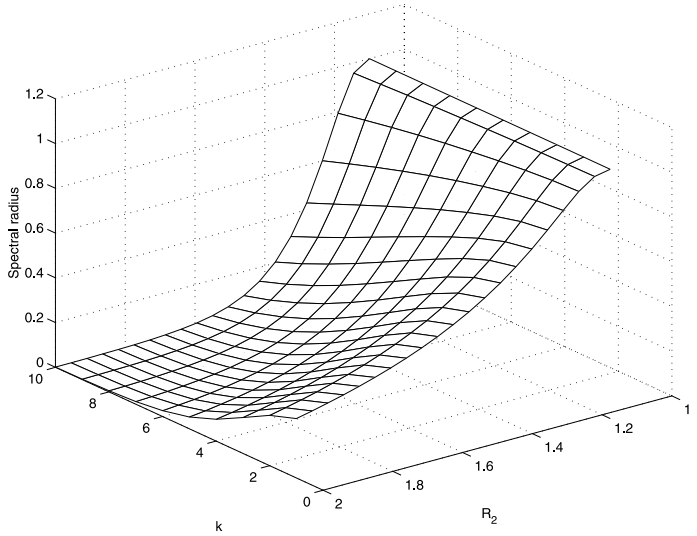

Fig. 2. Spectral radius of T_k as a function of k and R_2 when velocity is used as matching condition to update the coefficients on the outer cage. The inner cage is located at $R_1 = 1.1$ and the far-field boundary is located at $R_\infty = 5$.

sufficiently close to the cylinder for a given k to ensure convergence, it is more desirable to have the cage inside the cylinder and close to the cylinder surface in practice.

The effects of cage locations on the convergence rate of the method are summarized in Tables 1 and 2. In the case of using velocity matching, the best strategy is to place both cages outside the cylinder and

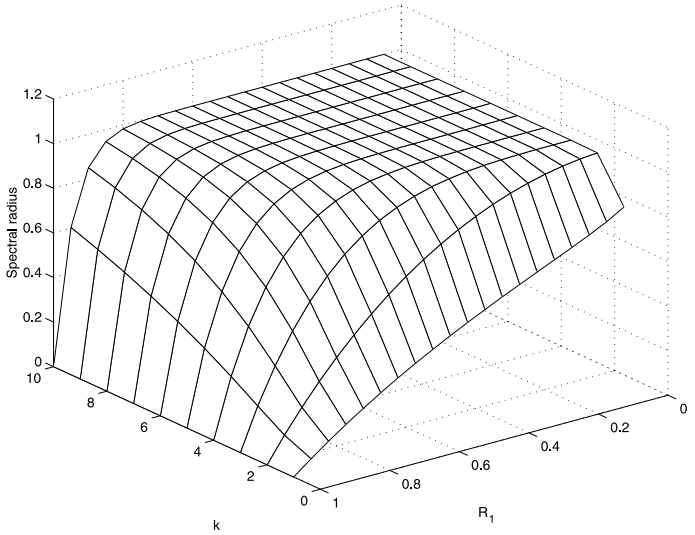

Fig. 3. Spectral radius of T_k as a function of k and R_1 when pressure and vorticity matching condition is used to update the coefficients on the outer cage, whose location is irrelevant in this case. The far-field boundary is located at $R_\infty = 5$ and inner cage is inside the cylinder with $0 < R_1 \leqslant 1$.

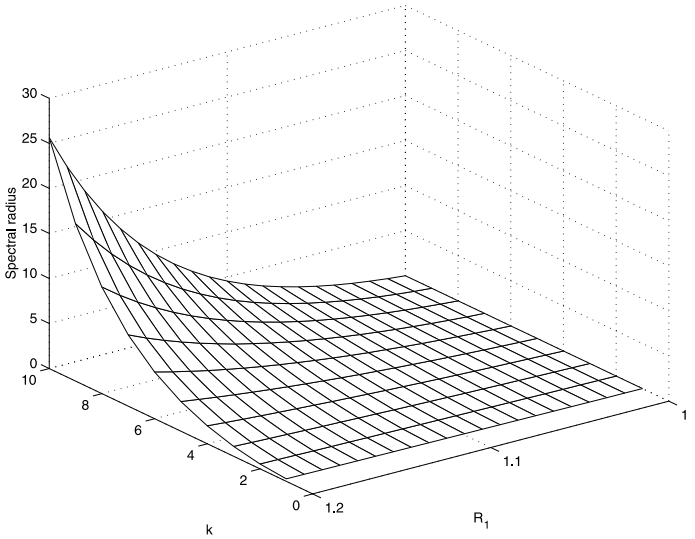

Fig. 4. Spectral radius of T_k as a function of k and R_1 when pressure and vorticity matching condition is used to update the coefficients on the outer cage, whose location is irrelevant in this case. The far-field boundary is located at $R_\infty = 5$ and the inner cage is outside the cylinder with $1 \leqslant R_1 \leqslant 1.2$.

Table 1
Illustration of convergence for Stokes flows using velocity matching

	$R_2 \leqslant R_1$	$R_2 > R_1$ ($R_2 \approx R_1$)	$R_2 \gg R_1$
$R_1 \leqslant 1$	Diverges	Diverges	Diverges
$R_1 > 1$	Diverges	Converges (slow)	Converges (fast)

Table 2
Illustration of convergence for Stokes flows using pressure/vorticity matching

$R_1 \ll 1$	$R_1 \approx 1$	$R_1 \gg 1$
Converges (slow)	Converges (fast)	Diverges

maintain some distance between them. In other words, one should avoid placing both cages too close to the cylinder surface. When the pressure and vorticity are used as matching conditions, however, it is desirable to place the inner cage as close to the cylinder surface as possible while the location of the outer cage is irrelevant.

4. Conclusion

In this paper we have investigated the convergence property of PHYSALIS when it is applied to solve the Laplace and biharmonic equations using circular cages. To simplify the analysis, we have assumed circular geometry and that the far-field solution (solution between the inner cage and the far-field boundary) can be obtained exactly. In practice, the far-field solution is obtained numerically. For example, in [14], a fractional step method on a staggered grid is used to find the outer solution.

In general, we found that the convergence for the Laplace equation is robust if proper matching conditions are used on the inner and outer cages. In the context of potential flows, the best strategy is to use the normal velocity on the inner cage to compute the far-field solution and update the coefficients of the eigenfunction expansion of the local solution by matching the velocity potential on the outer cage. Convergence can be achieved as well if the velocity potential is used on both cages while the speed of convergence is slower in this case.

The situation is more complicated for the biharmonic equation. In the context of Stokes flows, when the velocity is used as matching condition on the outer cage to update the coefficients of the local solution (eigenfunction expansion), convergence becomes slow when the cages are close to the cylinder and the method does not converge when the cages are inside the cylinder or for a single cage case. Since the real interest of using PHYSALIS is for computing the incompressible flows governed by the Navier–Stokes equations, and the analytical expression (eigenfunction expansion) is only valid near the particle surface, we are facing a dilemma. On one hand, we are required to set up the cages near the surface in order to use the eigenfunction expansion. On the other hand, convergence becomes slow when the cages are near the particle surface.

The convergence result for the pressure–vorticity matching condition is more interesting from practical point of view since the method converges when a single cage is used and the cage can be placed inside the cylinder. More importantly, the analysis indicates that convergence is faster when the cage is closer to the surface, which avoids the dilemma faced by the velocity matching conditions when the method is applied to the Navier–Stokes equations. Therefore, a fine grid is desirable as the cage is normally set up using the grid points next to the cylinder. The analysis also shows that the convergence is in general better when the cage is inside the cylinder than when it is outside. Slower convergence is expected for high frequency mode in the

local expansion solution, which suggests that the method works better for less oscillatory flows. Finally, we note that pressure and vorticity matching conditions can be used while the computation is carried out using either primitive variable formulation (velocity and pressure as primary unknowns) or the stream-function vorticity formaulation (in the two-dimensional case). In either case, vorticity or pressure needs to be computed based on the primary unknowns and some care should be taken to avoid the loss of accuracy. However this issue is not addressed in the present study.

Acknowledgements

The authors wish to thank Professor Andrea Prosperetti for many interesting discussions and helpful suggestions. This research is partially supported by the Natural Sciences and Engineering Research Council (NSERC) of Canada and the Japanese Ministry of Education.

References

[1] A. Ahmed, S. Elghobashi, Direct numerical simulation of particle dispersion in homogeneous turbulent shear flows, Phys. Fluids 12 (2000) 2906–2930.
[2] S. Chen, G. Doolen, Lattice Boltzmann method in fluid flows, Ann. Rev. Fluid Mech. 30 (1998) 329–364.
[3] C. Crowe, T. Troutt, J. Chung, Numerical models for two-phase turbulent flows, Ann. Rev. Fluid Mech. 28 (1996) 11–41.
[4] E.-J. Ding, C. Aidun, The dynamics and scaling law for particles suspended in shear flow with inertia, J. Fluid Mech. 423 (2000) 317–344.
[5] H.H. Hu, Direct simulation of flows of solid–liquid mixtures, Int. J. Multiphase Flow 22 (1996) 335–352.
[6] H.H. Hu, N.A. Patankar, M.Y. Zhu, Direct numerical simulation of fluid–solid systems using arbitrary Lagrangian–Eulerian technique, J. Comput. Phys. 169 (2000) 427–462.
[7] R. Glowinski, T.-W. Pan, T. Hesla, D. Joseph, A distributed Lagrange multiplier/fictitious domain method for particulate flows, Int. J. Multiphase Flow 25 (1999) 755–794.
[8] D. Koch, A. Ladd, Moderate Reynolds number flow through periodic and random arrays of aligned cylinders, J. Fluid Mech. 349 (1997) 31–66.
[9] A. Ladd, Sedimentation of homogeneous suspensions of non-Brownian spheres, Phys. Fluids 9 (1997) 491–499.
[10] N. Patankar, P. Singh, D. Joseph, R. Glowinski, T.-W. Pan, A new formulation of the distributed Lagrange multiplier/fictitious domain method for particulate flows, Int. J. Multiphase Flow 26 (2000) 1509–1524.
[11] A. Prosperetti, H.N. Oguz, PHYSALIS: a new o(N) method for the numerical simulation of disperse systems, Part I: potential flow of spheres, J. Comput. Phys. 167 (2001) 196–216.
[12] A. Sangani, G. Mo, An O(N) method for Stokes and Laplace interactions, Phys. Fluids 31 (1996) 2435–2444.
[13] A. Stock, Particle dispersion in flowing gases, J. Fluid Eng. 118 (1996) 4–17.
[14] S. Takagi, H.N. Oguz, Z. Zhang, A. Prosperetti, PHYSALIS: a new method for particle simulation, Part II: two-dimensional Navier–Stokes flows around cylinders, J. Comput. Phys. 187 (2003) 371–390.